

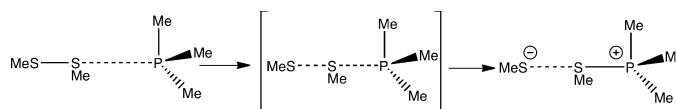
Mechanism of S_N2 Disulfide Bond Cleavage by Phosphorus Nucleophiles. Implications for Biochemical Disulfide Reducing Agents

Olga Dmitrenko, Colin Thorpe, and Robert D. Bach*

Department of Chemistry and Biochemistry, University of Delaware, Newark, Delaware 19716

rbach@udel.edu

Received June 13, 2007



The B3LYP variant of DFT has been used to study the mechanism of S–S bond scission in dimethyl disulfide by a phosphorus nucleophile, trimethylphosphine (TMP). The reaction is highly endothermic in the gas phase and requires significant external stabilization of the charged products. DFT calculations (B3LYP) were performed with explicit (water molecules added) and implicit solvent corrections (COSMO model). The transition structures for this S_N2 displacement reaction in a number of model systems have been located and fully characterized. The reaction barriers calculated with different approaches for different systems are quite close (around 11 kcal/mol). Remarkably, the calculations suggest that the reaction is almost barrierless with respect to the preorganized reaction complex and that most of the activation energy is required to rearrange the disulfide and TMP to its most effective orientation for the SMe group transfer way. Different reactivities of different phosphorus nucleophiles were suggested to be the result of steric effects, as manifested largely by varying amounts of hindrance to solvation of the initial product phosphonium ion. These data indicate that the gas-phase addition of a phosphine to the disulfide moiety will most likely form a phosphonium cation–thiolate anion salt, in the presence of four or more water molecules, that provide sufficient H-bonding stabilization to allow displacement of the thiolate anion, a normal uncomplicated S_N2 transition state is to be expected.

1. Introduction

Bimolecular nucleophilic substitution (S_N2) reactions are among the most widely used reactions in organic chemistry, and consequently, they have been studied extensively.^{1,2} An important subset of such basic transformations involves S–S bond cleavage in biochemistry and under typical laboratory conditions. The relative ease with which the S–S bond can be broken and reformed makes this area of chemistry both interesting and essential to a number of biochemical transformations. Indeed, the importance of thiol–disulfide interchange reactions to biochemistry have encouraged a variety of physical–organic investigations of the mechanism of this reaction.³ The remarkable ability of this mercaptide exchange process to effect reversible cleavage and formation of the S–S bond is exemplified by the enzymatic reactions carried out by the

oxidized and reduced states of the thioredoxin fold involving mixed disulfides.^{4,5} A kinetic study on thiolate–disulfide interchange using coenzyme A and cysteine with oxidized glutathione (GSSG) has been reported employing NMR spectroscopy.⁶ The rate constants for the thiolate anionic forms of Co-A and cysteine with GSSG again suggested that reduction of disulfides are mechanistically uncomplicated S_N2 reactions.

Experimental mechanistic studies on S–S bond scission where phosphorus is the nucleophile have received far less attention.³ Overman and co-workers⁷ suggested a two-step

(1) Shaik, S. S.; Schlegel, H. B.; Wolfe, S. *Theoretical Aspects of Physical Organic Chemistry. The S_N2 Mechanism*; Wiley: New York 1992.

(2) Lowry, T. H.; Richardson, K. S. *Mechanism and Theory in Organic Chemistry*, 3rd ed.; Harper and Row: New York 1987.

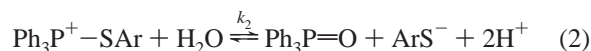
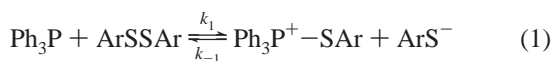
(3) Parker, A. J.; Kharasch, N. *Chem. Rev.* **1959**, 59, 583.

(4) (a) Holmgren, A. *Structure* **1995**, 3, 239. (b) Darby, N. J.; Freedman, R. B.; Creighton, T. E. *Biochemistry* **1994**, 33, 7937. (c) Wood, Z. A.; Poole, L. B.; Karplus, P. A. *Biochemistry* **2001**, 40, 3900. (d) Chivers, P. T.; Prehoda, K. E.; Raines, R. T. *Biochemistry* **1997**, 36, 4061.

(5) (a) Gross, F.; Sevier, C. S.; Vala, A.; Kaiser, C. A.; Fass, D. *Nature Struct. Biol.* **2002**, 9, 61. (b) Ellgaard, L.; Ruddock, L. W. *EMBO Rep.* **2005**, 6, 28. (c) Sevier, C. S.; Kaiser, C. A. *Antioxid Redox Signal* **2006**, 8, 797. (d) Nakamoto, H.; Bardwell, J. C. *Biochim. Biophys. Acta* **2004**, 1694, 111. (e) Wilkinson, B.; Gilbert, H. F. *Biochim. Biophys. Acta-Proteins Proteomics* **2004**, 1699, 35.

(6) Keire, D. A.; Strauss, E.; Guo, W.; Noszal, B.; Rabenstein, D. L. *J. Org. Chem.* **1992**, 57, 123.

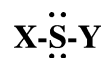
process for the attack of triphenylphosphine (Ph₃P) on a series of symmetrical aryl disulfides on the basis of a stopped-flow kinetic study. In the first step, it was proposed that the phosphorus atom attacked the sulfur along the S–S bond axis displacing a thiolate anion attending the formation of a thioalkoxyphosphonium cation (eq 1).



In a subsequent step, it was suggested that this cationic intermediate underwent hydrolysis to form the phosphine oxide and a second equivalent of thiolate anion (eq 2). This was a particularly interesting study for its time because of the potential for sulfur, a third-row element, to expand its valence shell. In this series of kinetic studies the initial attack by phosphorus on the S–S moiety was shown to be rate limiting but void of any discernible influence by neighboring group participation by substituents on the aryl group of the disulfide. Most of the kinetics studies reported by the Overman group⁷ were carried out in mixed or protic solvents. The observation that in aprotic solvents alkyl disulfides do not react with Ph₃P even after several hours at 140 °C has implications for biochemical processes and would seem to contradict the observations of Whitesides,⁸ who observed higher rates of thiolate–disulfide exchange in DMSO and DMF than in water. However, it is noteworthy that in this case the Ph₃P nucleophile does not bear a negative charge. Despite the fact that the reaction of phosphines with disulfides in the presence of water to produce thiols (eqs 1 and 2) had been known since 1935,⁹ this series of mechanistic studies has only recently led to a useful application of this S_N2 reaction largely because the commonly available phosphines are malodorous and have a limited solubility in water. This lack of utility was remedied by Whitesides, who found that tris(2-carboxyethyl)phosphine (TCEP) reduces disulfides rapidly and quantitatively in water at pH 5.¹⁰ This was a particularly important observation because this new disulfide reducing reagent could be readily prepared in large quantity by hydrolysis of its corresponding tris(2-cyanoethyl)phosphine (TCNP). It was proposed that this new disulfide cleavage reagent in biological systems followed the same mechanistic protocol involving a simple S_N2 attack at disulfide sulfur as suggested above (eqs 1 and 2). This water-soluble phosphine (TCEP) has become widely employed for the reduction of the disulfide linkage in a variety of peptides, proteins, and cellular systems.¹¹ TCEP has proven to be a useful complementary reagent to dithiothreitol (DDT) because it is air stable, and in contrast to DDT, it is an

irreversible reducing agent that cannot directly catalyze thiol–disulfide exchange reactions.

Since TCEP has recently become a widely accepted substitute for dithiothreitol (DDT), the efficacy of the mono-, di-, and triesters of TCEP were subsequently compared by Thorpe and co-workers¹² to that of DDT toward disulfide cleavage with a series of model disulfides including the disulfide bonds in thioredoxin and sulfhydryl oxidase. Esterification of TCEP was found to increase lipophilicity allowing the trimethyl ester, tmTCEP, to penetrate phospholipids bilayers rapidly in contrast to DDT that crosses membranes more slowly. Although these experimental studies have done much to define the reactivity and utility of both thiolates and phosphines as effective nucleophiles toward disulfides, very little is known about the activated complex for this series of S_N2 displacement reactions. In particular, it is not yet understood whether these reactions actually proceed by an addition–elimination mechanism or in some cases if a concerted displacement takes place in the absence of a discrete intermediate. This is especially problematic for a third-row element, like sulfur, because hypervalent sulfur complexes¹³ with 10 valence electrons



formally a sulfurane albeit with two lone-pairs of electrons, are quite stable and can correspond to a local minimum on the potential energy surface (PES) for the S_N2-like trisulfide anionic TSs. The question of whether such structures are actually a local minimum or a saddle point becomes the primary issue in a theoretical study of such transformations.¹⁴ It was suggested on the basis of CCSD and DFT calculations that the transition state for RS[−] attack on RS–SR proceeds in most cases by a trianionic [^δ–S–S–S^{δ−}] structure, although the energy of the corresponding minimum attending an addition–elimination mechanism was very close in energy.¹⁵

To date, we have found no systematic theoretical study of the attack of phosphorus on the disulfide linkage. In a recent theoretical study,¹⁶ we reexamined the nature of the intermediate-transition structure for the S_N2 attack of CH₃S[−] on dimethyl disulfide at several levels of theory including CCSD¹⁷ and determined the effect of solvation on this thiol–disulfide

(7) (a) Overman, L. E.; Matzinge, D.; O'Connor, E. M.; Overman, J. D. *J. Am. Chem. Soc.* **1974**, *96*, 6081. (b) Overman, L. E.; Petty, S. T. *J. Org. Chem.* **1975**, *40*, 2779. (c) Overman, L. E.; O'Connor, E. M. *J. Am. Chem. Soc.* **1976**, *98*, 771.

(8) (a) Houk, J.; Whitesides, G. M. *J. Am. Chem. Soc.* **1987**, *109*, 6825. (b) Singh, R.; Whitesides, G. M. *J. Am. Chem. Soc.* **1990**, *112*, 1190. (c) Singh, R.; Whitesides, G. M. *J. Am. Chem. Soc.* **1990**, *112*, 6304.

(9) Schönberg, A. *Chem. Ber.* **1935**, *68*, 163.

(10) Burns, J. A.; Butler, J. C.; Moran, J.; Whitesides, G. M. *J. Org. Chem.* **1991**, *56*, 2648.

(11) (a) Han, J. C.; Han, G. Y. *Anal. Biochem.* **1994**, *220*, 5. (b) Gray, W. R. *Protein Sci.* **1993**, *2*, 1732. (c) Getz, E. B.; Xiao, M.; Chakrabarty, T.; Cooke, R.; Selvin, P. R. *Anal. Biochem.* **1999**, *273*, 73. (d) Geiger, L. K.; Kortuem, K. R.; Alexejun, C.; Levin, L. A. *Neuroscience* **2002**, *109*, 635. (e) de Lamiande, E.; Gagnon, C. *Free Radical Biol. Med.* **1998**, *25*, 803.

(12) Cline, D. J.; Redding, S. E.; Brohawn, S. G.; Psathas, J. N.; Schneider, J. P.; Thorpe, C. *Biochemistry* **2004**, *43*, 15195.

(13) (a) For earlier discussions concerning the nature of chemical bonding in hypervalent molecules, see: Reed, A. E.; Schleyer, P. v. R. *J. Am. Chem. Soc.* **1990**, *112*, 1434. (b) An excellent discussion of revised models for hypervalent bonding may be found in: Dobado, J. A.; Martinez-Garcia, H.; Molina, J. M.; Sundberg, M. R. *J. Am. Chem. Soc.* **1990**, *112*, 8461.

(14) (a) For complimentary theoretical investigation of classical S_N2 attack at carbon versus silicon, see: Bento, A. P.; Sola, M.; Bickelhaupt, F. M. *J. Comput. Chem.* **2005**, *26*, 1497. (b) For explanations concerning those steric factors involved in the disappearance of the central barrier for S_N2 attack at silicon see: Bento, A. P.; Bickelhaupt, F. M. *J. Org. Chem.* **2007**, *72*, 2201. (c) For a thorough theoretical analysis of the origin of the disappearance and reappearance of reaction barriers for S_N2 attack at phosphorus see: van Bochove, M. A.; Swart, M.; Bickelhaupt, F. M. *J. Am. Chem. Soc.* **2006**, *128*, 10738.

(15) (a) Bachrach, S. M.; Mulhearn, D. C. *J. Phys. Chem.* **1996**, *100*, 3535. (b) Bachrach, S. M.; Hayes, J. M.; Dao, T.; Mynar, J. L. *Theor. Chem. Acc.* **2002**, *107*, 266. (c) Bachrach, S. M.; Pereverzev, A. *Org. Biomol. Chem.* **2005**, *3*, 2095. (d) Hayes, J. M.; Bachrach, S. M. *J. Phys. Chem.* **2003**, *107*, 7952. (e) Bachrach, S. M.; Chamberlin, A. C. *J. Org. Chem.* **2003**, *68*, 4743. (f) Bachrach, S. M.; Gailbreath, B. D. *J. Org. Chem.* **2001**, *66*, 2005.

(16) (a) Bach, R. D.; Dmitrenko, O.; Thorpe, C. *J. Org. Chem.* To be submitted. (b) Glukhovtsev, M. N.; Bach, R. D.; Pross, A.; Radom, L. *Chem. Phys. Lett.* **1996**, *160*, 558.

interchange using the COSMO^{17d} solvent model in addition to the inclusion of explicit waters of solvation. These results provide a unique contrast to the use of phosphorus as the nucleophile and the role of the recently developed phosphorus reducing agents for the disulfide moiety.

2. Computational Methods

Ab initio molecular orbital calculations were performed with the Gaussian 98 and 03 programs.^{17a,b} The Becke three-parameter hybrid functional combined with the Lee, Yang, and Parr (LYP) correlation functional, denoted B3LYP,¹⁸ was employed in the calculations using density functional theory (DFT). In this study, we used 6-31G(d) and 6-311+G(d,p) basis sets. Optimization of all structures used the Berny algorithm¹⁹ and the keyword MODREDUNDANT.^{17a,b} Additional bond distances (e.g., H-bonding interactions) were included as explicit variables when they typically were over 2 Å. Some additional bond angles, not treated specifically, and especially dihedral angles involving H-bonds were added between the four heavy atoms omitting the hydrogen atom. This dampens the displacements, cutting down on wagging and bending motions, and typically reduces the number of gradient cycles by up to one half. The B3LYP variant of DFT theory does provide reasonable values of complexation energies for ion–dipole complexes formed in prototypical gas-phase S_N2 reactions of halide anions attacking saturated carbon [Cl[−] + CH₃Cl].^{16b} However, the overall Δ*H* barriers for these reactions are typically underestimated when compared to G2(+) calculations or experimental data. A more recent evaluation of S_N2@C versus S_N2@Si reactions also suggests that the B3LYP variant of DFT underestimates reaction barriers relative to CCSD(T)/aug-cc-pVQZ calculations.^{14a} Recently developed DFT method using the OLYP variant appear to give slightly better results than B3LYP for S_N2 reaction barriers. The partial charges were calculated using the NBO method²⁰ implemented in the Gaussian program.

Corrections for solvation (single-point calculations on gas-phase optimized structures) and optimizations in dielectric medium with the water dielectric constant (ε = 78.39) were made using the polarizable conductor COSMO^{17d} method in Gaussian G98.^{17a} Bond dissociation energies were based upon enthalpies calculated at the B3LYP/6-311+G(d,p) level and, in selected cases, the G3^{21a} method have been used. As indicated by our earlier studies, B3LYP-calculated PA are typically 2–3 kcal/mol lower than PAs calculated at the G2 level,²² which provides excellent agreement with experiment.

Most of the calculations were performed using GridChem computational resources and services, Computational Chemistry Grid²³ (www.gridchem.org).

3. Results and Discussion

(a) S–S versus P–S Bond Dissociation Energies. Prior theoretical studies by Bachrach¹⁵ on thiol–disulfide exchange

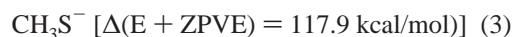
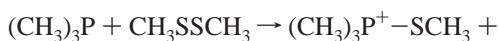
TABLE 1. Calculated Bond Dissociation Energies (Δ*H*₂₉₈, kcal/mol)

| compound | Δ <i>H</i> ₂₉₈ |
|--|---|
| HS–SH | 61.6 ^c [G3], 56.8 ^d [B3LYP/6-31+G(d)] |
| CH ₃ S–SCH ₃ | 50.7 ^c [B3LYP/6-311+G(d,p)] 54.7 ^d [B3LYP/6-31+G(d)] 64.8 ^c [CBS-Q], 63.1 ^c [G3], 63.8 ^f [exp] |
| (CH ₃) ₃ P ⁺ –SCH ₃ | 70.2 ^c [B3LYP/6-311+G(d,p)], 87.3 ^c [G3] |
| (CH ₃) ₂ P–SCH ₃ | 67.4 ^c [G3] |

^a Reference 24d. ^b Reference 24a. ^c This work. ^d Reference 25. ^f Reference 26.

have pointed to the difficulties in distinguishing between S_N2 processes involving a transition state or an addition–elimination (A–E) reaction where a discrete long-lived intermediate can be identified on the reaction pathway. We have examined the question of the expansion of the valence shell of the sulfur atom under attack^{16a} and in the present study the thermodynamics of S–S versus P–S bond making/breaking in these displacement reactions. We have estimated the S–S versus the P–S bond dissociation energies (BDE) for the two reactions (Table 1). Although a series of O–O BDEs have been recently reported, accurate S–S bond energies have only recently been made available.^{16a} At the G3 level, which should provide BDE within chemical accuracy, we find the S–S bond in HS–SH to be comparable in magnitude to the S–S bond in CH₃S–SCH₃ (63.1 kcal/mol). A comparison of S–S vs P–S BDE show the latter to be 3.6 kcal/mol (G3) stronger when both compounds are neutral. However, the P–S bond appears to be much stronger (87.3 kcal/mol) when P–S bond formation is associated with the formation of a formal positive charge on the phosphorus (P⁺–S). It is difficult to gauge the effect of electrostatic interactions upon homolytic cleavage of this P–S bond.

(b) S_N2 Reactions with the S–S Bond Involving Phosphorus as the Nucleophile. An S_N2 reaction at the S–S bond involving a neutral phosphorus compound differs markedly from the same process described above involving thiolate anion. One of the challenging features of the gas-phase reaction of a phosphine (PR₃) with a disulfide is the fact that while the reactants are neutral, the products on the right side of the equation are charged species (eq 3). It is obvious that without solvent stabilization, the developing ionic species in the gas-phase reaction will be highly endothermic as a result of Coulombic effects. For example, at the B3LYP/6-311+G(d,p) level, isolated products are 117.9 kcal/mol higher in energy than reactants (eq 3).



In addition, the developing P⁺–S bond along the reaction coordinate is much stronger than the relatively weak S–S bond (63.1 kcal/mol) that is being cleaved. While experimental data for the P–S bond strength are limited, we calculate this BDE to be 67.4 kcal/mol (G3) for the neutral P–S bond in (CH₃)₂P–SCH₃. However, we *estimate* the P⁺–S bond for the phosphonium salt [(CH₃)₃P⁺–SCH₃] to be 19.9 kcal/mol stronger at

(22) Bach, R. D.; Thorpe, C.; Dmitrenko, O. *J. Phys. Chem. A* **2002**, *106*, 4325.

(23) (a) Milfeld, K.; Guiang, C.; Pamidighantam, S.; Giuliani, J. Proceedings of the Linux Clusters: The HPC Revolution. (b) Dooley, R.; K. Milfeld, K.; Guiang, C.; Pamidighantam, S.; Allen, G. Proceedings of the Global Grid Forum 14, 2005.

(17) (a) Frisch, M. J. et al. *A. Gaussian 98*, revision A.7; Gaussian, Inc.: Pittsburgh, PA, 1998. (b) Gaussian 03, revision B.05 (SGI64–G03RevB.05); Gaussian, Inc.: Pittsburgh, PA, 2003. See the Supporting Information for the full list of authors. (c) Barone, V.; Cossi, M. *J. Phys. Chem. A* **1998**, *102*, 1995. (d) Barone, V.; Cossi, M.; Tomasi, J. *J. Comp. Chem.* **1998**, *19*, 404.

(18) (a) Becke, A. D. *Phys. Rev. A* **1988**, *37*, 785. (b) Lee, C.; Yang, W.; Parr, R. G. *Phys. Rev.* **1988**, *B41*, 785. (c) Becke, A. D. *J. Chem. Phys.* **1993**, *98*, 5648. (d) Stevens, P. J.; Devlin, F. J.; Chabowski, C. F.; Frisch, M. J. *J. Phys. Chem.* **1994**, *80*, 11623.

(19) Gonzalez, C.; Schlegel, H. B. *J. Chem. Phys.* **1989**, *90*, 2154.

(20) (a) NBO Version 3.1, Glendening, E. D.; Reed, A. E.; Carpenter, J. E.; Weinhold, F. (b) Carpenter, J. E.; Weinhold, F. *THEOCHEM* **1988**, *169*, 41. (c) Foster, J. P.; Weinhold, F. *J. Am. Chem. Soc.* **1980**, *102*, 7211. (d) Reed, A. E.; Curtiss, L. A.; Weinhold, F. *Chem. Rev.* **1988**, *88*, 899.

(21) (a) Curtiss, L. A.; Raghavachari, K.; Redfern, P. C.; Rassolov, V.; Pople, J. A. *J. Chem. Phys.* **1998**, *109*, 7764. (b) Curtiss, L. A.; Raghavachari, K.; Trucks, G. W.; Pople, J. A. *J. Chem. Phys.* **1991**, *94*, 7221.

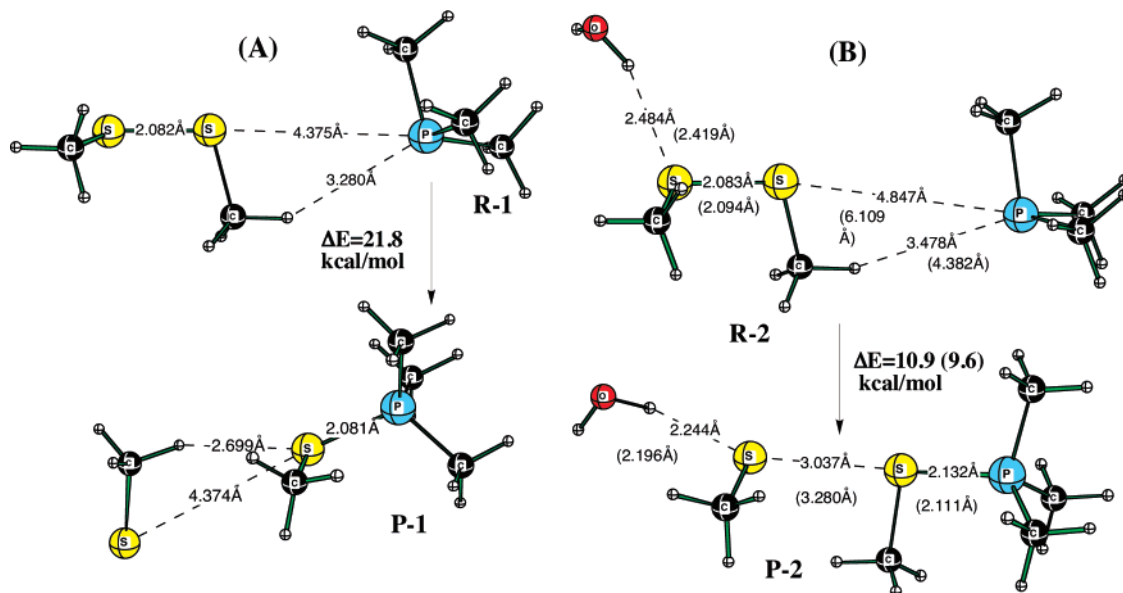


FIGURE 1. (A) Reactant complex $[(CH_3)_3P^+ \cdots CH_3SSCH_3]$, **R-1** and product $[(CH_3)_3P^+ - SCH_3 \cdots CH_3S^-]$, **P-1** complex optimized in water media (COSMO method) at the B3LYP/6-31G(d) level of theory. (B) Reactant complex $[(CH_3)_3P^+ \cdots CH_3SSCH_3 \cdots H_2O]$, **R-2** and product $[(CH_3)_3P^+ - SCH_3 \cdots CH_3S^- \cdots H_2O]$, **P-2** complexes optimized in water media using the COSMO protocol and B3LYP/6-31G(d) and B3LYP/6-311+G(d,p) basis sets (numbers in parentheses).

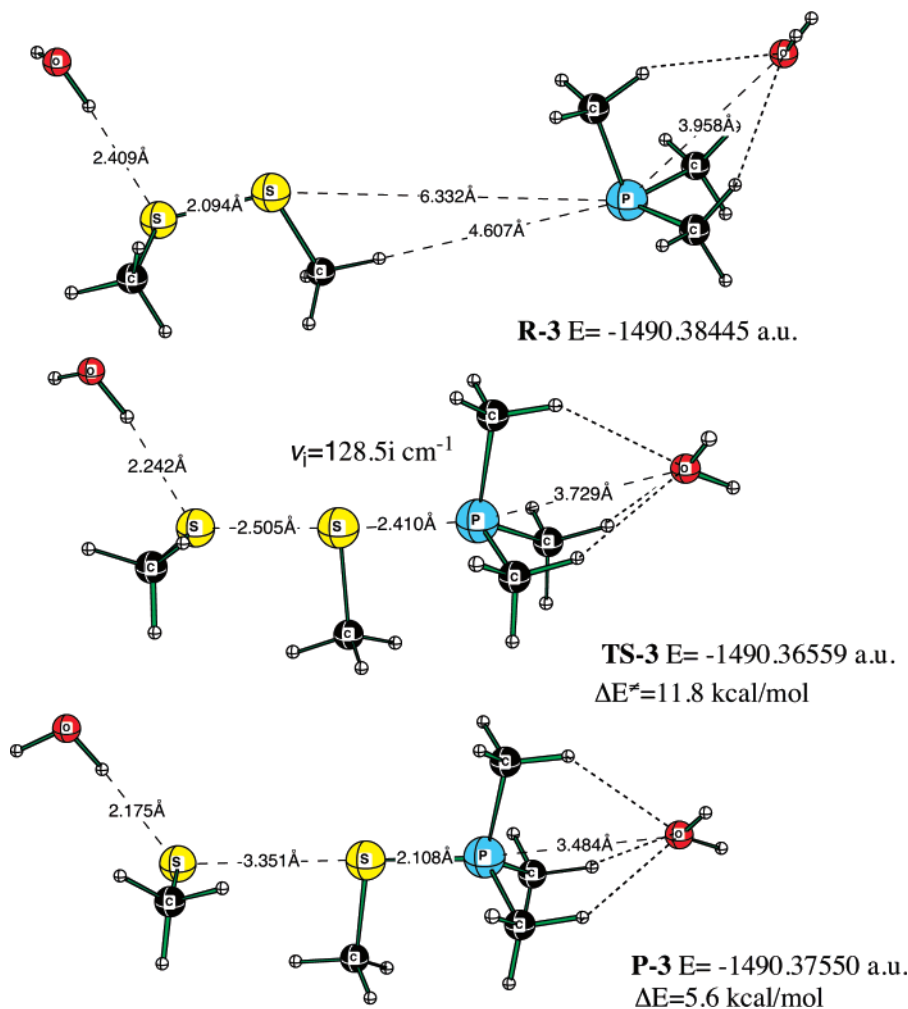


FIGURE 2. Reactant complex $[H_2O \cdots (CH_3)_3P^+ \cdots CH_3SSCH_3 \cdots H_2O]$, **R-3**, transition structure **[TS-3]**, and the product complex $[H_2O \cdots (CH_3)_3P^+ - SCH_3 \cdots CH_3S^- \cdots H_2O]$, **P-3** optimized in water media using the COSMO method at the B3LYP/6-311+G(d,p) level of theory.

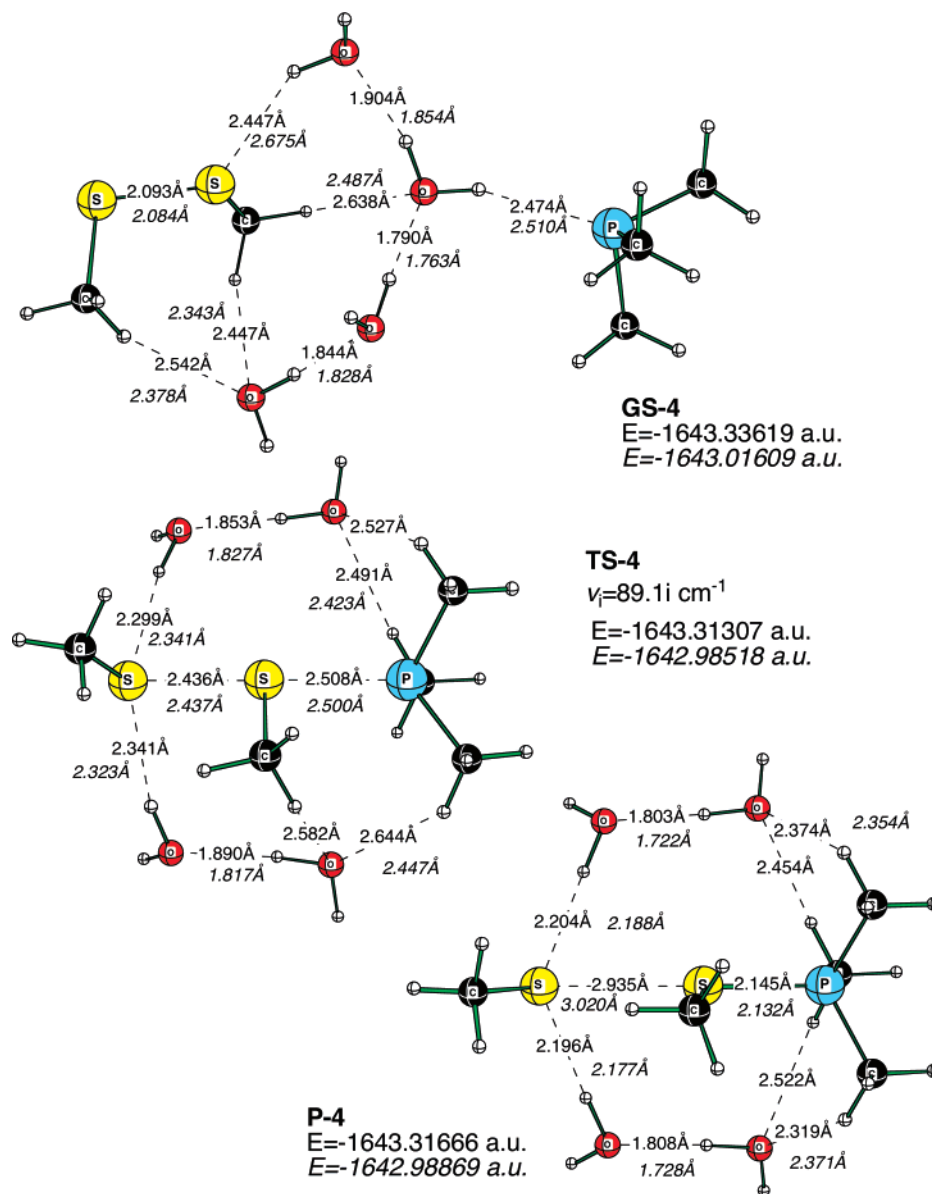


FIGURE 3. Stationary point structures for the reaction of trimethylphosphine with dimethyl sulfide assisted by four water molecules optimized in the gas phase at the B3LYP/6-311+G(d,p) level of theory. Numbers in italics correspond to the B3LYP/6-31G(d) optimizations.

the G3 level (Table 1). While this difference in BDE would normally portend an exothermic reaction with bond making preceding bond breaking, this potential energetic consequence is thwarted by the charge separation attending the breaking of the S–S bond and the departing thiolate anion.

The prospect of developing charge in the TS (eq 3) prompted us to do geometry optimizations in dielectric media (water) using the COSMO^{17d} method to assess the effect of solvation on the overall energetics of the reaction. We were able to locate complexation minima for both the reactants and products on the potential energy surface (PES), but a transition structure for this S–S bond cleavage could not be found (Figure 1 A). The failure to locate a TS and the relatively high endothermicity of the reaction (21.8 kcal/mol, B3LYP/6-31G(d)) stimulated us to specifically solvate the reactant with one water molecule in order to stabilize the leaving group through a hydrogen bond to the developing CH_3S^- leaving group anion. The endothermicity of this reaction dropped to 10.9 kcal/mol at the B3LYP/

6-31G(d) level reflecting the H-bonding energy of the water molecule (Figure 1B).

Calculations with a more flexible basis set [6-311G+(d,p)] results in a similar endothermicity, $\Delta E = 9.6$ kcal/mol, but neither reaction proceeded through a discernible TS. Thus, in spite of the changes in the geometrical parameters of both complexes, the larger basis set has little effect upon the energetics. Although addition of just one water molecule to the model system was not sufficient to facilitate location of a TS, when a second water was positioned near the phosphonium cation $(\text{CH}_3)_3\text{P}^+-\text{SCH}_3$, in a way that allows $\text{C}-\text{H}\cdots\text{OH}_2$ hydrogen bonding involving the $(\text{CH}_3)_3\text{P}$ methyl groups (Figure 2), a TS does exist. Remarkably, one can see in Figure 2 how the distance between the phosphorus atom and oxygen of the added water molecule becomes shorter along the reaction coordinate (it changes from 3.96 Å in R to 3.48 Å in P), which clearly indicates the important role of phosphonium cation stabilization by solvent. The same is true for the SCH_3^- anionic

side. At the B3LYP/6-311G+(d,p) level, this water-assisted reaction [2H₂O] has an endothermicity of 5.6 kcal/mol and a barrier of 11.8 kcal/mol. The transition structure for this S_N2 displacement reaction has a characteristic imaginary frequency, 128.5i cm⁻¹ [B3LYP/6-31G(d)], which can be visualized as vibrational movement of the central S–CH₃ moiety between the terminal S and P atoms. We reiterate that location of the TS with two specific waters of solvation was achieved using the COSMO protocol.

Since the COSMO solvation model does not explicitly treat hydrogen bonding, we carried out a series of calculations on the S_N2 attack of a phosphine on the S–S linkage with explicit treatment of water molecules in the *absence of the COSMO solvation model*. We started with inclusion of one water molecule and extended this explicit solvation shell to include a larger number of water molecules, *N*. At *N* < 4, we were unable to locate the either the product complex or the TS in contrast to the aforementioned TS that could be located in water media (COSMO). For example, in the case involving two water molecules H-bonded to the leaving thiolate, we had to impose a constraint on the developing P–S bond (to its approximate value in the product). This allowed us to estimate the endothermicity of this displacement to be about 25 kcal/mol. In this series of reactions the first successful location of a TS required the involvement of four water molecules. Optimization (*N* = 4) of **TS-4**, (Figure 3) evidenced the formation of two water bridges between the phosphine and leaving thiolate. The same structural feature is observed in product cluster, **P-4**, while the reactant minimum **GS-4** has a different organization of the H-bonded water network.

Interestingly, with the smaller basis set, we first located prereaction complex **R-4** (Figure 4), which has the bridged water network similar to **TS-4** and **P-4**. Re-optimization with the 6-311+G(d,p) basis set resulted in a deeper minimum, **GS-4** which also could be found at the B3LYP/6-31G(d) level of theory (Figure 4). IRC calculations (B3LYP/6-31G(d)) confirmed that **R-4** and **P-4** are the minima connected directly to **TS-4** on the PES. Thus, with respect to pre-organized reaction complex **R-4**, the reaction barrier is 5.8 kcal/mol [B3LYP/6-31G(d)+ZPVE]. The total reaction barrier should be calculated from the global minimum, which may not necessarily be **GS-4** because deeper minima with a different organization of water molecules may exist. This exercise serves to demonstrate the importance of employing polarization functions when addressing questions of hydrogen bonding.

We used **GS-4** to estimate reaction energetics and effects of solvent and basis sets (Table 2). From the results for B3LYP/6-31G(d)-optimized structures (columns 1, 3, and 4 in Table 2), one can see that about 70–80% of the energy contribution to the reaction barrier is due to the structural re-organization of **GS-4** to prereaction complex, **R-4**. Remarkably, the reaction barriers calculated with different approaches for different systems, B3LYP/6-311+G(d,p)+COSMO (Figure 1) and B3LYP/6-311+G(d,p) +COSMO(solvent = water)//B3LYP/6-31G(d) (Table 2, fourth column), are quite close, 11.8 and 10.9 kcal/mol.

We also performed gas-phase optimizations of the transition structures with larger numbers of water molecules (*N* = 5–7). These data are given in the Supporting Information. The largest TS that we have been able to optimize is for *N* = 8 (Figure 5). As one may expect, it is an earlier transition structure than in

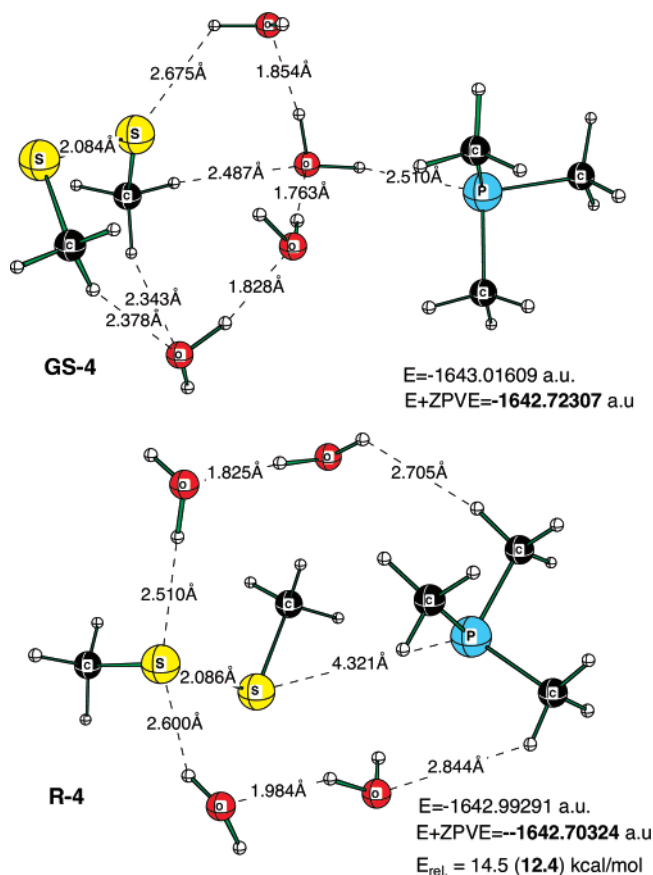


FIGURE 4. B3LYP/6-31G(d)-optimized structures of reactant complexes, global minimum (**GS-4**), and prereaction complex (**R-4**). Energies in bold are calculated with zero-point vibrational energies (ZPVE).

TABLE 2. Reaction Energetics for Dimethyl Disulfide S–S Bond Cleavage with Trimethylphosphine Assisted by Four Water Molecules^a

| | B3LYP/ SB | B3LYP/ MB | B3LYP/MB// B3LYP/SB | B3LYP/MB+ COSMO(water)// B3LYP/SB |
|-------------|----------------------|----------------------|------------------------|---|
| GS-4 | 0 | 0 | 0 | 0 |
| R-4 | 14.5 (12.4) | - | 9.8 | 8.9 |
| TS-4 | 19.4 (18.3) | 14.5 (13.9) | 14.4 | 10.9 |
| P-4 | 17.2 (16.7) | 12.3 (12.4) | 11.3 | 2.0 |

^a Bold numbers in parentheses are calculated with ZPVE corrections. Here, SB is the 6-31G(d) basis set, and MB is the 6-311+G(d,p) basis set.

the case with *N* = 4: The S–S distance is shorter and the S–P distance is longer in **TS-5** (Figure 5) vs **TS-4** (Figure 3).

In order to get an idea about the effect of the length of water bridges, we report here the results for the system with *N* = 6 water molecules that forms 2 bridges similar to the case with *N* = 4 discussed above and shown in Figures 3 and 4. In this type of approach there are undoubtedly many more ways to orient the water molecules but we attempted to maintain a somewhat symmetrical array of hydrogen bonds to the reactants. The only directly connected stationary points (**R-6**, **TS-6**, and **P-6**) on the PES have been optimized and are given in Figure 6. The introduction of a water molecule into each bridge in the case of the *N* = 6 system resulted in a tighter contact of reactants (S...P distance decreased from 4.321 to 3.493 Å, Figures 3 and 5) which contrasts to expectations that the lengthening of the bridges will allow a more relaxed and looser complex. **TS-6** is earlier than **TS-4** which is evidenced by a shorter S–S

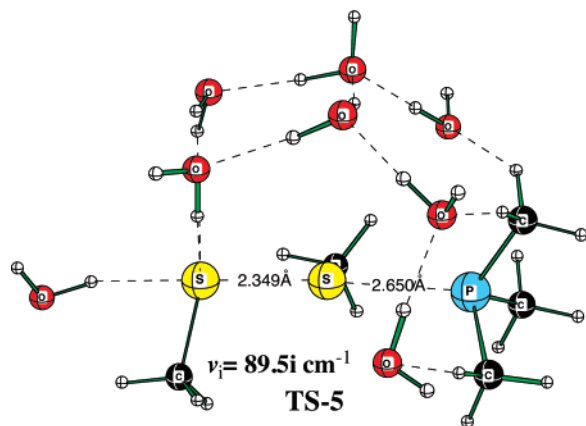


FIGURE 5. B3LYP/6-31G(d)-optimized transition structure with eight water molecules, **TS-5**.

distance (2.375 vs 2.436 Å). And, finally, the **P-6** complex is less tightly bound (S...S distance is 3.156 Å in **P-6** and 2.935 Å in **P-4**) and the S–P bond in the cation is shorter (2.145 vs 2.110 Å). From these geometrical changes one may expect a lower reaction barrier and deeper product minimum. A comparison of the energetics for both systems summarized in Table 3 supports this assumption. In terms of local minima directly connected to the TS, **R** and **P**, gas-phase B3LYP/6-31G(d)+ZPVE calculations indicate that the reaction becomes slightly exothermic for $N = 6$ whereas at $N = 4$, it is endothermic (first and second columns, Table 3). The single-point solvent corrections with the larger basis set [B3LYP/6-311+G(d,p) + COSMO//B3LYP/6-31G(d), third and fourth columns, Table 3] lead to rather unpredictable results; the barrier is now lower for $N = 4$ but the exothermicity is larger for $N = 4$ as well. This contradictory observation can be understood through the charge distribution analysis given in Figure 7. Smaller charges are developed in the TS in case of the 6-water system (numbers in brackets) vs the 4-water system. This would suggest that the 6-water TS should be more stable and earlier than the 4-water TS. Interestingly, in both systems, the transferring SCH₃ group is almost neutral in the transition structure.

From these collective data we may conclude that while the gas-phase addition of a phosphine to the disulfide moiety will most likely form a phosphonium cation–thiolate anion salt, in the presence of four or more water molecules, that provide sufficient H-bonding stabilization to allow displacement of the thiolate anion, a normal uncomplicated S_N2 transition state is to be expected.

(c) Relative Reactivity of Biochemically Important Disulfide Reducing Agents. We next address the question of why tris(2-cyanoethyl)phosphine (TCNP) exhibits a surprisingly slow kinetic behavior toward a series of disulfides, while tris(2-carboxyethyl)phosphine (TCEP) and its corresponding trimethyl ester, tmTCEP, rapidly reduce S–S bonds.^{10,12} First we examined some of the physical properties of TCNP and found, rather surprisingly, that the p*K* of this tertiary phosphine was reported to be only 1.36 while the acidity of protonated (CH₃)₃P was 8.65, a typical value for a trialkylphosphine.^{27a} Second, the

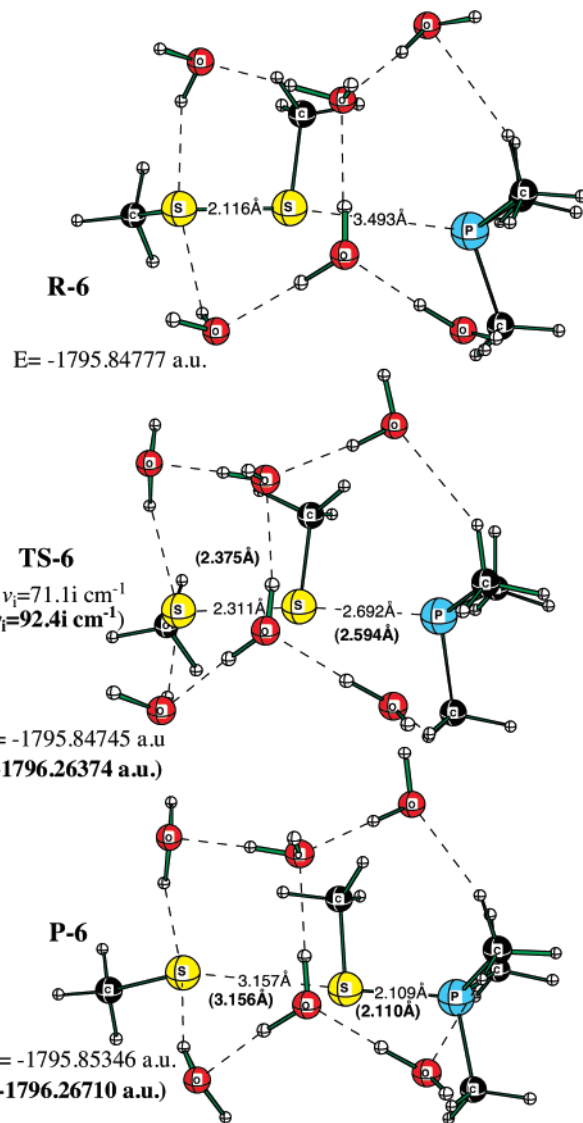


FIGURE 6. Stationary points structures for the reaction of trimethylphosphine with dimethyl sulfide assisted by six water molecules optimized in the gas phase at the B3LYP/6-31G(d) level of theory. Bold numbers in parentheses correspond to the B3LYP/6-311+G(d,p) optimizations.

TABLE 3. Comparison of the Reaction Energetics for Disulfide S–S Bond Cleavage with Trimethylphosphine Assisted by Four and Six Water Molecules on the Part of PES That Is Directly Connected to the TS (**R** and **P** are Prereaction and Postreaction Local Minima)

| | B3LYP/SB + ZPVE | | B3LYP/MB + COSMO//B3LYP/SB | |
|-----------|-----------------|---------|----------------------------|---------|
| | $N = 4$ | $N = 6$ | $N = 4$ | $N = 6$ |
| R | 0 | 0 | 0 | 0 |
| TS | 5.8 | 1.0 | 2.0 | 2.8 |
| P | 4.2 | −1.4 | −6.9 | −5.1 |

relative nucleophilicity of TCNP toward alkyl halides in a typical S_N2 reaction was shown to be atypically low.^{27b} The rate ratio for the S_N2 reaction of TCNP versus CH₃P toward ethyl iodide

(24) (a) Bach, R. D.; Ayala, P. Y.; Schlegel, H. B. *J. Am. Chem. Soc.* **1996**, *118*, 12758. (b) Bach, R. D.; Dmitrenko, O.; Estévez, C. M. *J. Am. Chem. Soc.* **2005**, *127*, 3140. (c) Estevez, C. M.; Dmitrenko, O.; Winter, J. E.; Bach, R. D. *J. Org. Chem.* **2000**, *65*, 8629. (d) Bach, R. D.; Dmitrenko, O. *J. Phys. Chem. B* **2003**, *107*, 12851.

(25) Jursic, B. S. *Int. J. Quant. Chem.* **1997**, *62*, 291.

(26) Price, C. C.; Oae, S. *Sulfur Bonding*; Ronald Press: New York, 1962.

(27) (a) Henderson, W. A., Jr.; Streuli, C. A. *J. Am. Chem. Soc.* **1960**, *82*, 5791. (b) Henderson, W. A., Jr.; Buckler, C. A. *J. Am. Chem. Soc.* **1960**, *82*, 5794.

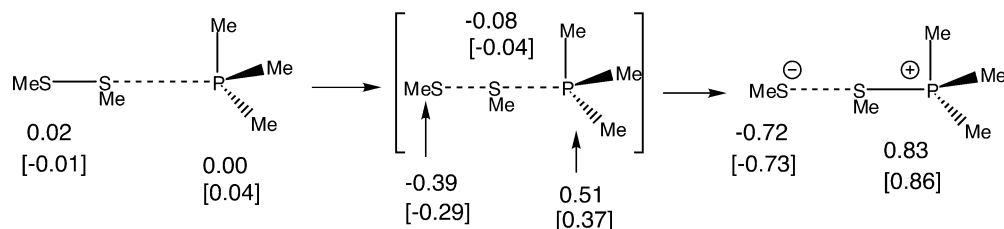


FIGURE 7. NBO charge distribution (electrons) calculated for B3LYP/6-31+G(d,p)-optimized stationary points for the systems with four and six water molecules (numbers in brackets).

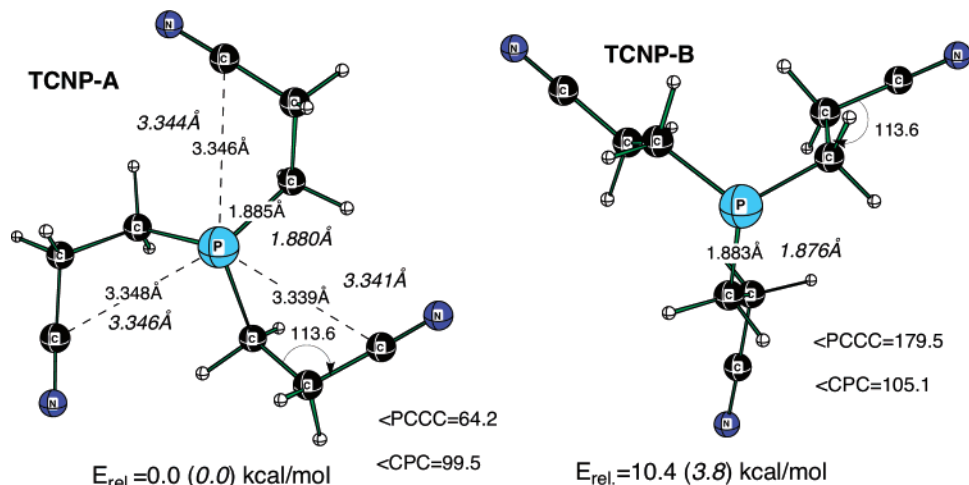


FIGURE 8. Two conformers of tris(2-cyanoethyl)phosphine, TCNP-A and TCNP-B, optimized at the B3LYP/6-31G(d) level of theory in gas phase (plain numbers) and in water (italic numbers) using the COSMO model. The conformer relative energies (E_{rel} , kcal/mol) are based upon sum of electronic and zero-point energies.

TABLE 4. Calculated NBO Charge on P (electrons), Dipole Moments (μ , Debye) Proton Affinities (kcal/mol) for TCPN-A and TMP at the B3LYP/6-31G(d) (A), B3LYP/6-311+G(d,p) (B) Levels and in Water [COSMO, B3LYP/6-311+G(d,p)//B3LYP/6-311+G(d,p)] (C)^a

| compd | NBO charge on P | dipole μ_{neutral} | PA(A) | PA(B) | PA(C) |
|--------|-----------------|-------------------------------|-------|-------|-------|
| TCPN-A | 0.8406 | 1.91 | 213.4 | 210.1 | 270.0 |
| TCPN-B | 0.8905 | 2.28 | 205.1 | | |
| TMP | 0.8504 | 1.24 | 227.1 | 225.4 | 284.5 |
| TCEP | 0.8856 | 1.87 | 225.1 | | |

^a PA values are based upon enthalpies.

in acetone was 3×10^{-3} . A weak interaction of the phosphorus atom with the β -nitrile group was offered as a possible explanation for the lower reactivity of TCNP. It was also noted in that study that the rate of these S_N2 reactions were notably faster in more polar solvents consistent with what we have found in the present study.

Initially, we performed conformational searches for both reducing agents. At least two distinct conformations can be found (Figure 8) in gas phase and in water for the tricyano reducing agents TCNP-A and TCNP-B. The cyclic-like conformation for TCNP-A is most likely a global minimum since it has smaller dipole moment (Table 4).

The basic differences between TCNP-A and TCNP-B are the P–C–C–CN dihedral angles. In TCNP-A, dihedral angle $\angle\text{PCCC} = 64.5^\circ$ provides a suitable geometry for a potential P–CN interaction. The dihedral angle in the TCNP-B conformer (179.5°) tends to direct the CN moiety away from the P atom.

The energy separation between TCNP-A and TCNP-B becomes smaller in water media due to a larger stabilization of

conformer B with the higher dipole moment. One may suggest that in TCNP-A global conformer there are three specific interactions between C=N and the P atom that make phosphorus less nucleophilic. In other words, the above interactions, which are specific to the TCNP-A conformer and absent in the TCEP phosphine, are responsible for the poor activity with respect to S–S bond cleavage. Surprisingly, there is not much difference in the NBO charge distribution for both conformers (Table S1, Supporting Information). In accord with the electronegativity of the requisite elements involved (for P, C and N the electronegativity is 2.1, 2.5 and 3.0), in both TCNP conformers the largest positive charge (NBO) is on the P atom (0.841 and 0.891 electrons in conformers A and B), and the terminal CN nitrogens are negatively charged [–0.332 (A) and –0.307 (B) electrons]. This makes the dipole moment of the TCNP-A extended conformation somewhat larger.

A comparison of the calculated proton affinities for TCNP and TMP (Table 4) suggests that TCNP is markedly less basic and therefore perhaps less nucleophilic. The TCNP-A affinity toward a proton is almost 15 kcal/mol lower than in the case of TMP. Interestingly, the lowest PA was found for TCNP-B, which can be understood in view of the largest dipole moment change upon protonation (Table 4). The protonated TCNP-A (cation) is 19.0 kcal/mol more stable than protonated TCNP-B. This suggests that one possible origin for the poor kinetic behavior of TCNP is that conformer TCNP-A resists the angular motion required to make it more pyramidal in its protonated form. The force constants for changes in the bond angles around a tertiary phosphine are known to be quite high. Inversion of configuration at a nitrogen atom is quite facile while the stereogenic center in a chiral phosphorus compound is resolvable

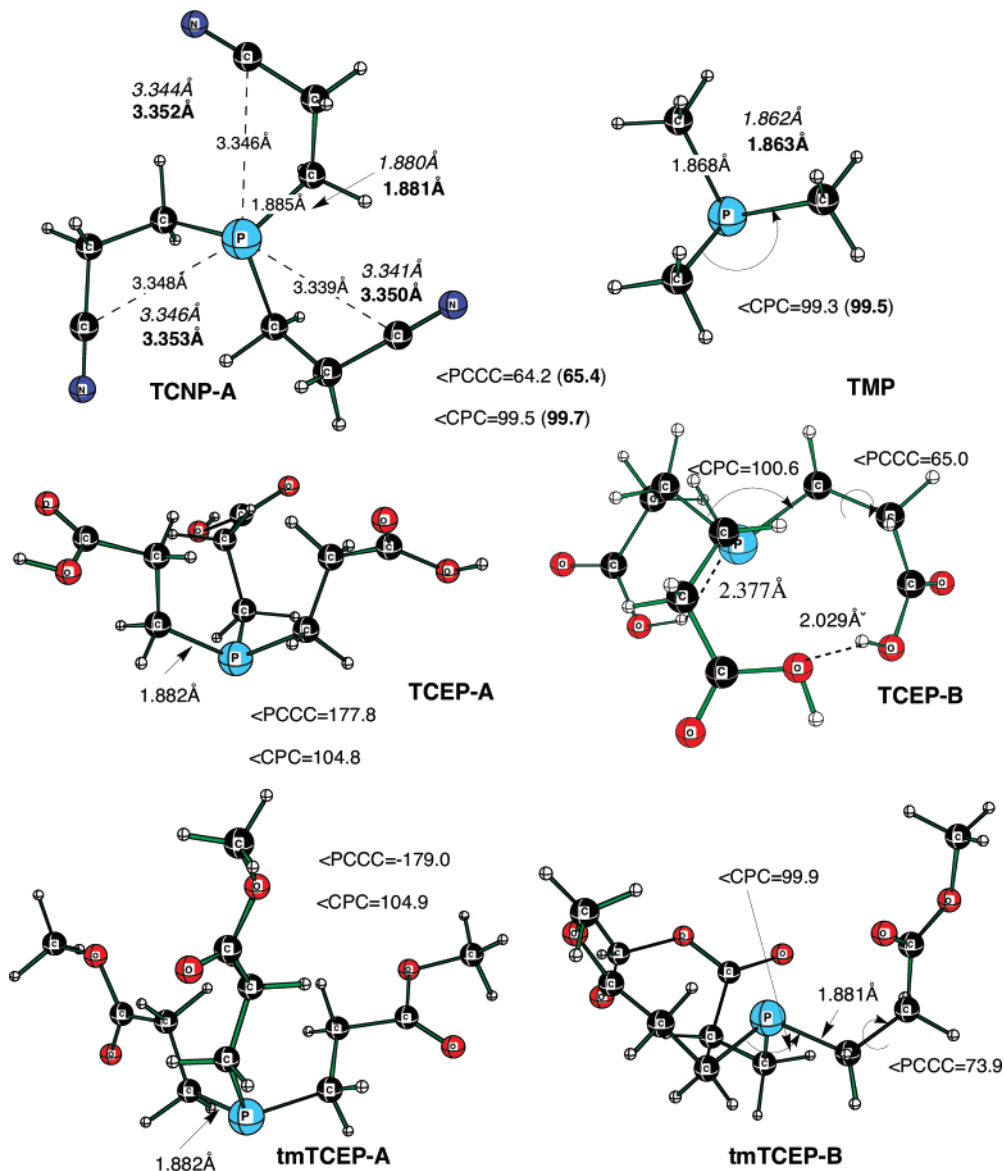
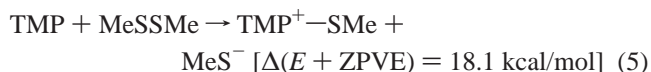
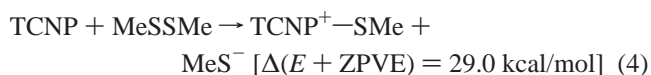


FIGURE 9. Two conformers each of tris(2-cyanoethyl)phosphine (TCNP), trimethylphosphine (TMP), tris(2-carboxyethyl)phosphine (TCEP), and the trimethyl ester of TCEP (tmTCEP) (optimized at the B3LYP/6-31G(d) level of theory in gas phase (plain numbers) and in water (italic numbers) using the COSMO solvent model. Numbers in bold for TCNP correspond to gas-phase B3LYP/6-311+G(d,p)-optimized structures.

into its two enantiomers. For example, the calculated inversion barrier in trimethylamine is 6.40 kcal/mol while that in trimethylphosphine is 41.2 kcal/mol [B3LYP/6-31+G(d,p)]. Since we sensed that these phosphines were resisting the opportunity to become pyramidal upon S_N2 attack at sulfur, we estimated the inversion barriers by making the phosphorus planar with approximate C–P–C bond angles of 120° . Geometry optimization until all forces (but not displacements) were converged resulted in energy increases of 30, 27 and 32 kcal/mol for tmTCEP, TCPN-B, and TCPN-A. As noted above for the calculated PA, it is TCPN-A that appears to resist becoming pyramidal and we attribute this to some form of interaction of the P atom with the nitrile functional group.

The same suggestion about the low TCPN reactivity can be deduced from a comparison of the reaction energetics (eqs 4 and 5) characterized by the energy differences between reactant and product complexes fully optimized at the B3LYP/

6-31G(d) level of theory (TCNP-A was used in these calculations).



In contrast to TCPN-A, the C–P–C bond angles in the TCEP phosphine global minimum (Figure 9, TCEP-A) suggest that it may not experience great difficulty upon protonation consistent with its much greater PA and its greater reductive power toward the S–S bond.

It has been proffered, in the older literature,²⁷ that the basicity of phosphines is largely determined by inductive effects as

measured by $\Sigma\sigma^*$ with deviations from this analysis being the result of steric effects. Although it is well-established that pentacoordinate phosphorus species play a key role in such displacement reactions, it remains difficult to distinguish stable intermediate complexes from labile transition states (TS). A recent systematic theoretical comparative study of S_N2@C, S_N2@Si, and S_N2@P reactions has established with some conviction that increasing the coordination number around the P atom, as well as, steric effects shift the mechanism back to a double well potential mechanism (TS) that more closely resembles a typical S_N2 reaction at carbon.^{14c}

In the present case, steric effects, as manifested largely by varying amounts of hindrance to solvation of the product phosphonium ion, would appear to provide a very likely explanation for the rather puzzling lack of reactivity of TCNP toward the disulfide linkage in biochemical reactions. In fact, TCNP has the lowest p*K*_a of an entire series of 16 tertiary phosphines trialkylphosphines including (*cyclo*-C₆H₁₁)₃P that has a p*K*_a of 9.7. Unlike the case for amines, where solvation is invariant or largely negligible for tertiary amines but very important for primary and secondary amines, where the role of the N–H bond in hydrogen bonding is important, this solvation effect is still operative for tertiary phosphines. Thus, the geometry of the developing phosphonium ion upon TCNP attack, at the rather hindered tertiary structure of an S–S linkage in a protein, does not relax sufficiently for those reasons delineated above, to allow adequate solvation of the salt product. This provides a rather unique explanation why TCNP is so sluggish in its S_N2 reactivity toward disulfides and TCEP is much more reactive. Although TCNP has been proposed to be a potentially useful reducing agent for buried disulfides, it exhibits surprisingly slow kinetic reactivity. For example, second-order rate constants for TCNP are 30-fold slower than those of TCEP toward 5,5'-dithio(2-nitrobenzoic acid (DTNB). This is likely a reflection of the very low p*K*_a of TCNP at phosphorus (≈1.4).¹²

The lowest energy conformer of TCEP-A (Figure 9) has the three COOH groups down and away from the P atom with P–C–C–C=O dihedral angles averaging 176.5° (TCEP-A). The bond angles around phosphorus are approaching tetrahedral (105°) and the P atom is appropriately exposed to engage in an S_N2 attack at sulfur. If the P–C–C–C=O dihedral angles are rotated (average 68.7) to place the COOH above the plane of the P atom (TCEP-B) this conformer is 2.5 kcal/mol higher in energy despite the fact that one of the COOH groups is within H-bonding distance of the P atom (H...P = 2.38 Å) and a second strong H-bond (2.02 Å) exists between two of the COOH groups. Thus, the COOH groups, while not essential to S–S

bond cleavage,¹² are solvated and oriented in such a fashion as to enhance its nucleophilicity.

Esterification of TCEP does exert a modest effect upon the p*K*_a at phosphorus. Mono-, di-, and trimethyl esters exhibit p*K*_a values of 6.8, 5.8, and 4.7, respectively, extending their reactivity with model peptides to correspondingly lower pH values relative to that of the parent TCEP (p*K*_a = 7.6).¹² In fact, at Ph 5.0 the order of reactivity is reversed and tmTCEP is 35-fold more reactive than TCEP. The lower energy conformer of tmTCEP-A has all three P–C–C–C=O dihedral angles nearly 180° in such a manner where the phosphorus is approaching tetrahedral (104.9°) and the P atom is exposed for the S_N2 attack at sulfur. Conformer tm-TCEP-B, where we have arranged the ester carbonyl carbon atoms in a manner where they could potentially interact with the P atom in a manner suggested for the CN moiety in TCNP, is 6.3 kcal/mol higher in energy. In this case, the P–C–C–C=O dihedral angles average 72.9° with the three C–P–C angles about phosphorus being considerably less than tetrahedral (99.9°). The P atom is sterically hindered in this conformer essentially excluding it from being involved in S–S bond cleavage. The P atom carbonyl carbon distances are 3.38 Å, which is only 0.04 Å longer than those in TCNP-A yet in the ester case we find this to be the higher energy conformer. It is also known that increasing the steric demand of the substituents around silicon can change the S_N2@Si mechanism from a stable single well intermediate to the normally encountered TS evidenced with S_N2@C reactions. This now appears to be a well-established behavior of third-row elements.

In summary, gas-phase S_N2 attack of a tertiary phosphine on a typical disulfide linkage will most likely proceed through phosphonium cation intermediate with formation of a salt-like complex involving the displaced thiolate anion (eq 1). In protic solvents, where sufficient H-bonding is available to stabilize the departing thiolate anion, a typical uncomplicated S_N2 pathway (TS) is to be anticipated.

Acknowledgment. This work was supported by NIH GM26643 and partially supported by the National Computational Science Alliance under CHE050085 and CHE050039N and utilized the NCSA IBM P690 and NCSA Xeon Linux Supercluster. GridChem is also acknowledged for computational resources (www.gridchem.org) (see ref 23).

Supporting Information Available: Total energies and Cartesian coordinates. This material is available free of charge via the Internet at <http://pubs.acs.org>.

JO071271W